Desalination 344 (2014) 219–227

Contents lists available at ScienceDirect

Desalination

journal homepage: www.elsevier.com/locate/desal

# Structural optimization of seawater desalination: II novel MED–MSF–TVC configurations

Tawfiq H. Dahdah [a], Alexander Mitsos [a,b,*]

[a] Department of Mechanical Engineering, Massachusetts Institute of Technology, 77 Massachusetts Avenue, Cambridge, MA 02139, USA
[b] AVT Process Systems Engineering (SVT), RWTH Aachen University, Turmstrasse 46, Aachen, 52064, Germany

## HIGHLIGHTS

- We structurally optimize combined thermal desalination/ thermal compression systems.
- We model a superstructure allowing various vapor extraction options for compression.
- Intermediate vapor compression results in higher GOR and lower SA requirements.
- Optimal location of vapor extraction is heavily dependent on GOR requirement.
- We propose an integrated MED-TVC + MED + MSF system and a MED-TVC + MSF system.

## ARTICLE INFO

*Article history:*
Received 17 December 2013
Received in revised form 17 March 2014
Accepted 19 March 2014
Available online 17 April 2014

*Keywords:*
Desalination
Superstructure
Hybrid thermal desalination systems
Multi-objective optimization
MED
Thermal vapor compression

## ABSTRACT

A multi-objective structural optimization of integrated thermal desalination and thermal compression systems is performed, whereby the performance ratio of the structures is maximized while the specific area requirements are minimized. With the aid of the superstructure developed in part I, herein the thermal compression of vapor streams produced in intermediate multi-effect distillation (MED) effects as opposed to the common practice of compressing vapors produced in the last effect, is examined. The study concludes that intermediate vapor compression results in significant reductions in area requirements, as well as significant increases in maximum distillate production capacities. Moreover, the optimal location of vapor extraction is heavily dependent on the exact distillate production requirement in question. Two novel configuration forms are informed by the optimization. The first is an integrated MED–TVC + MED + MSF system, while the second is an integrated MED–TVC + MSF system.



## 1. Introduction

The overwhelming need to overcome the world-wide problems relating to water scarcity has motivated diverse investigations aiming to enhance existing thermal desalination technologies. Recently, multi-effect distillation–thermal vapor compression (MED–TVC) systems with a top brine temperature lower than 70 °C have been gaining heightened attention as a potential improvement over the conventional MED structures [1–3,5–8].

The relative superiority of such integrated structures is especially noticeable in cogeneration schemes where only medium to high pressure heating streams (2–15 bar) are available from pre-existing power plants [9,10]. In the most deployed MED–TVC scheme, a steam ejector utilizes the high pressure steam – known in this configuration as the motive steam – to entrain and subsequently compress a portion of vapor produced in the last MED effect. The resulting mixture, characterized by an intermediate pressure, is inputted as heating steam to the MED portion of the integrated plant, where it drives distillate production. For a fixed availability of motive steam at a specified pressure, this arrangement allows for the design of plants characterized by significantly larger distillate production capabilities (due to increased heating steam flow), coupled with reduced cooling water requirements on a per unit distillate basis [11]. This is in contrast to traditional MED plants which, constrained by the low temperature operation required to minimize scaling, are unable to notably benefit from the higher exergy source, which implies an inefficient use of motive steam. Additional cited advantages include moderate investment costs, high reliability, and easy operation and maintenance [12].

Several steady-state mathematical models of the aforementioned MED–TVC desalination system have been developed as in [13–18].

* Corresponding author at: AVT Process Systems Engineering (SVT), RWTH Aachen University, Turmstrasse 46, Aachen 52064, Germany.
*E-mail address:* amitsos@alum.mit.edu (A. Mitsos).

http://dx.doi.org/10.1016/j.desal.2014.03.026

These models were predominantly used to perform optimization studies seeking to determine preferable operating and design conditions for the system. Such investigations include examining the effect of factors such as the brine and intake seawater conditions, the number of effects, motive steam pressure and temperature, and the entrainment ratio on the total achievable distillate production of the plant. Other studies, however, have sought to fully optimize MED–TVC systems. Contrasting approaches include economic-based optimizations [10,19–21], thermodynamic optimizations [2,3,22] and thermoeconomic optimizations [23–25]. In these studies, the main variables that are modified by the optimization process are the top brine temperature, the entrainment ratio and the temperature differences between the effects. The structure of the thermal desalination plants, which informs how all the differing system flows are directed, are fixed prior to optimization. Most commonly a parallel feed MED (PF-MED) arrangement whereby equal feed is inserted into each of the effects is assumed, as in [14,3,11]. Another is the forward feed MED (FF-MED). Yet another is the parallel cross MED (PC-MED). Moreover, while there are numerous modes of integrating the steam ejector with the thermal desalination system, most authors have narrowed their focus on optimizing schemes where the steam ejector compresses the vapors produced in the last effect of the MED.

One excellent study by Bin Amer [3] proposes such an alternate scheme whereby the steam ejector is used to compress a portion of the vapor produced in an intermediate effect, while the remainder of the vapor is used to drive another series of MED effects. The benefits of compressing vapor generated in an intermediate vapor is confirmed in a subsequent study by Koukikamali et al. [26] who, using a parametric study, conclude that the middle effects are better positions to locate the suction port of the thermo-compressor in order to increase the gain output ratio and decrease the specific area. In both these studies, the routing of the flows is preset by the designers.

It is anticipated that the optimal flowsheet of the thermal desalination configuration – as part of an integrated system involving TVC – is different from that corresponding to a stand-alone thermal desalination configuration. Moreover, it is predicted that the optimal flowsheet highly depends on the location of vapor extraction. To the authors' knowledge, no optimization studies where the structure of the configurations in itself is a variable under investigation have already been carried out, although Zak [4] pointed to the importance of such an optimization work. This motivates the study proposed herein.

This article examines the advantages of intermediate thermal vapor compression by assessing its influence on several key parameters pertaining to both thermodynamic efficiency and economics. By doing so, desirable system characteristics, such as the optimal location of vapor extraction, the optimal quantity of vapor to entrain and optimal ejector compression ratio, are pinpointed. The overall goal is to propose alternate improved integrated structures, possibly of unconventional flow patterns, that are capable of maximizing the synergistic benefits of combining thermal desalination systems with thermal vapor compression systems.

**Table 1**
Choice of parameters for present study including motive steam and seawater conditions. Note that the vapor temperature to the first effect is not fixed, but rather determined by these parameters.

| Parameter | Value |
|---|---|
| Motive steam flowrate (kg/s) | 10 |
| Motive steam pressure (bar) | 15 |
| Seawater temperature (°C) | 25 |
| Seawater salinity (g/kg) | 4.2 |

## 2. Problem definition

For fixed seawater conditions, the optimization problem proposed herein is to identify the optimal integrated configuration given a fixed flow-rate of motive steam available at a pre-determined pressure. The choice of these input parameters is presented in Table 1, although the study could be easily replicated for alternate choices of these parameters. In determining the optimal structure, the optimization problem is to determine all of the variables presented below:

- The choice of hardware components;
- The routing of brine, feed and vapor flows within the system;
- The sizing of the components including the effects and feed preheaters;
- The pressure within each of the effects and flash boxes;
- The choice of how much vapor to entrain in an ejector; and
- The pressure of entrained vapor.

Section 3 presents the model developed for the sake of this optimization, while Section 4 details the characteristics of the optimization, including the solvers used in addition to both the choice of objective functions and imposed constraints.

## 3. Modeling

To enable the optimization procedure intended for this study, a flexible model of the integrated desalination and thermal compression plant is constructed. Note that the model corresponds essentially to standard models in literature. Such a model is adequate for the aim of this article, i.e., a methodology for structural optimization and identification of interesting potential structures. Substantially improving the model accuracy would result in a significantly more complicated model; this would change little in our methodology but present an optimization problem which is most likely intractable with state-of-the-art optimizers. Subsection 3.1 presents a graphic illustration of the superstructure used to represent the different possible thermal desalination structures allowed in this paper. Subsection 3.2 details the methodology used to integrate the thermal desalination model with the steam ejector, depending on choice of vapor extraction. Finally, Subsection 3.3 details the mathematical model used to represent the performance of the steam ejector, detailing in the process the constraints required to satisfy proper operation.

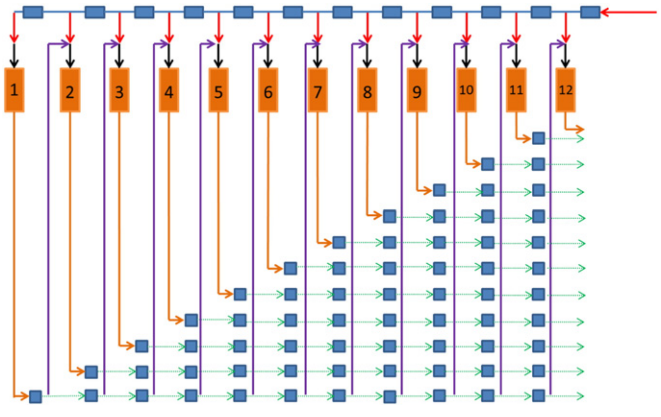


**Fig. 1.** Superstructure capable of representing different combinations of MSF, MED and feed preheater combinations. Vapor routings are not represented in this schematic.

### 3.1. The thermal desalination superstructure

The thermal desalination superstructure utilized in this work is represented in Fig. 1. While the superstructure can be used to represent any number of repeating units, the particular superstructure utilized in this work considers the specific example of 12 repeating units. Each theoretical unit is comprised of an effect, a preheater, a distillate flash box (not shown in figure for simplicity) and a set of brine flash boxes. It is important to clarify that just because a superstructure can represent a particular component does not mean that this particular component will be present in the finalized optimal structure. In fact, it will be observed in the Results and discussion section, that only a subset of allowable components is usually necessary. Manipulation of the component set in use is in principle controlled by the decision of what flow enters each component coupled with the decision of how to divide flows leaving a particular component. A detailed description of the different allowed flow options can be found in part I of this two-part paper.

Ultimately, a very large amount of structures can be represented through the proposed superstructure. These not only include prevalent configurations such as the FF-MED and PC-MED, but also include alternate non-conventional, yet potentially advantageous structures. Examples of potential structures include an MED structure that transitions to an MSF structure and a FF MED structure that transitions to a PC structure.

### 3.2. Integration with steam ejector

To allow investigating whether the entrainment of a particular vapor stream is justified, the superstructure discussed in part I of this paper is modified. Within the unit where the extraction occurs, the updated model accounts for the fact that only a fraction of the unit's generated vapor is used as heating steam to the next unit. Moreover, the model modifies the flow-rate of heating steam to the 1st effect to account for the addition of entrained vapor over and above the incoming motive steam.

Herein, only the thermal compression of vapors produced in the 4th, 6th, 9th and 12th (last) units is considered. While the analysis could be extended for vapors produced in any of the units, the proposed sample is sufficient to capture the dependence of the different variables on the location of vapor extraction. To this end, four different models are constructed based on mass, energy and species balances for each of the possible system components. Sample schematics illustrating how vapor redirection occurs are shown in Figs. 2 and 3.

### 3.3. Model of the steam ejector

One critical step in studying the performance of the integrated systems is the evaluation of the performance of the steam ejector. Although numerous steam ejector models exist in the literature including [27–30], the model used herein is based on the simple semi-empirical model proposed by El-Dessouky et al. [9,31]. This model, in turn, is based upon extensive field data for compression ratio and entrainment ratio gathered by Power [32]. The particular correlation is chosen since it avoids lengthy computations of correction factors, which are conditional upon the pre-availability of a detailed design of the ejector.

The used model determines the required mass of motive steam to compress a unit mass of suctioned vapor (a parameter known as the entrainment ratio (Ra)). Ra can be computed for any given motive steam pressure ($P_m$), suction pressure ($P_{ev}$), and desired discharge pressure ($P_s$) according to the relation below:

$$\mathrm{Ra}=\frac{M_m}{M_{ev}}=0.296\frac{(P_s)^{1.19}}{(P_{ev})^{1.04}}\left(\frac{P_m}{P_{ev}}\right)^{0.015}\left(\frac{3\times10^{-7}(P_m)^2-0.0009P_m+1.6101}{2\times10^{-8}(T_{ev})^2-0.0006(T_{ev})+1.0047}\right) \quad (1)$$

where $T_s$, $T_m$, and $T_{ev}$ refer to the temperatures, expressed in °C, of the discharge vapor streams, the motive steam and the entrained vapor respectively. All the pressure values are expressed in kPa.

El-Dessouky [9] further recommends the necessary conditions required to ensure normal, reliable and stable operation of the steam ejector. These are outlined below:

- $\mathrm{Ra} \leq 4$
- $10\ °\mathrm{C} \leq T_{ev} \leq 500\ °\mathrm{C}$
- $100\ \mathrm{kPa} \leq P_m \leq 3500\ \mathrm{kPa}$
- $1.81 \leq \mathrm{Cr} \leq 6$

where the compression ratio (CR) is defined as the pressure ratio of the discharge stream leaving the ejector to the vapor stream entrained in the ejector.

## 4. Optimization

### 4.1. Objective function

The profitability of operating a plant is of utmost importance when deciding to construct a particular plant. In desalination, the total generated revenue is dependent not only on the quantity of water produced, but also on the selling price of water. The main operating costs, on the other hand, are associated with the price of the total fuels required to supply heat to the thermal desalination plant. This in turn is dependent on local fuel costs, in addition to the quantity of fuel used. Finally the main capital costs are closely tied with the economics of construction of the flash boxes, the effects and the preheaters.

This paper does not seek to delve into a detailed economic study, for the simple reason that the economics are dependent on many factors

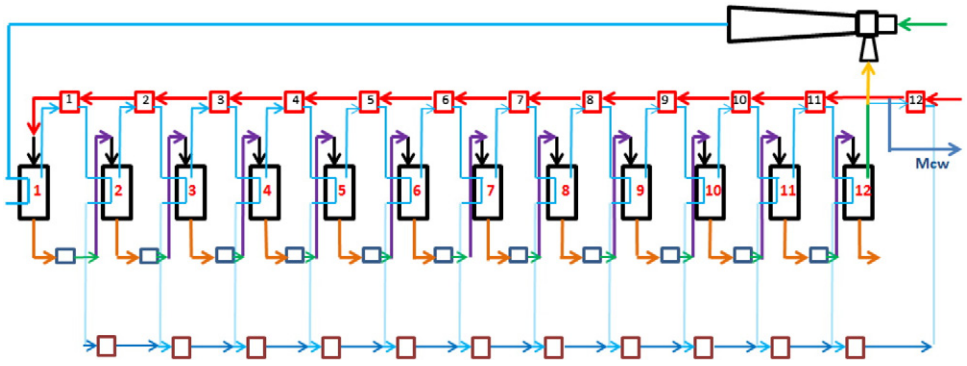


**Fig. 2.** Example of FF MED–TVC configuration with vapor extracted from last effect. Only a fraction of the vapor generated in last unit needs to be condensed in the down-condenser.

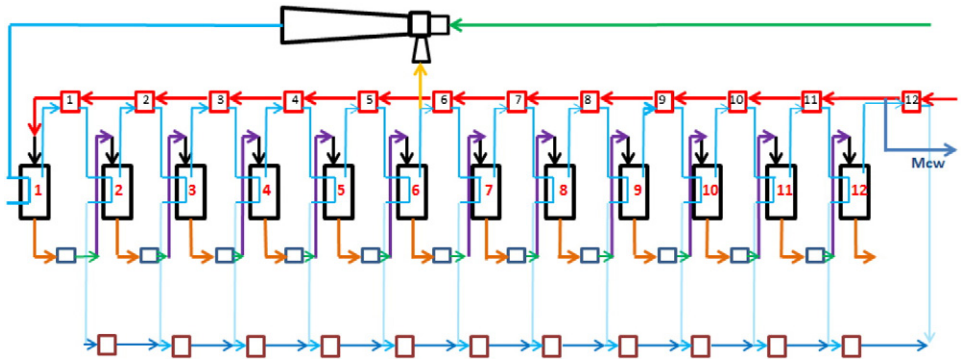


**Fig. 3.** Example of a FF MED–TVC with vapor extracted from an intermediate (6th) effect. Only a fraction of vapor produced in the 6th unit is directed towards feed pre-heating and vapor production within the next (7th) unit.

that are location-dependent and time-variant. Moreover, even the economic models already developed are acknowledged to have a high degree of uncertainty [17,3]. Instead, price-independent performance metrics are used in this work to allow comparison of different structures. The first metric used is the gain output ratio (GOR), defined as the mass ratio of the total distillate production in the plant to the total input motive steam. Since the pressure of the motive steam is fixed in this study, the GOR is a useful metric which can directly gauge the thermodynamic efficiency of a structure by quantifying distillate production from a fixed exergy input. In essence, the GOR relates the revenue generated in a plant to the operational costs associated with making steam available. The second metric is the specific heat transfer area requirements (SA), defined as the total heat transfer area (within effects, feed preheaters and the down condenser) per unit distillate. The parameter approximates required capital investments to construct a plant. The drawback of the parameter is that it inherently assumes that the cost of heat transfer areas within an effect and preheater is similar. It does however account for tradeoffs; for instance, a flash chamber at a low temperature results in high specific volume need but low heat transfer area need in effects and feed preheater.

Literature ultimately compares different plants, which differ in both their production capabilities alongside their area requirements, thus rendering comparison between structures very cumbersome. A particular structure may result in higher GOR whereas another may require lower SA. To counter this problem, herein multi-objective optimization is performed whereby the GOR is maximized while the SA is minimized. A Pareto frontier is constructed which informs designers of the minimum SA for each GOR requirement. It is left to the designer to decide which of the numerous Pareto-optimal points is preferable.

### 4.2. Optimization methodology

For each of the 4 models constructed, the multi-objective optimization approach implemented herein is approximated in a number of discrete steps. In each step the GOR is fixed prior to optimization, and SA is minimized for. The process is repeated for a range of GOR values. This rigorous approach is based on [35,36]. This discretization procedure is successful in reducing the problem to a series of single objective function optimization, thus enabling the use of black box solvers. All the models in this paper are developed in the General Algebraic Modeling System (GAMS), and globally optimized using BARON, a deterministic global algorithm capable of solving mixed integer non-linear programming problems [33,34]. Note that altogether the method guarantees the global solution of the optimization problems and thus the Pareto frontier; this cannot be guaranteed using stochastic algorithms such as evolutionary multiobjective optimizers.

### 4.3. Constraints to allow justified comparison of different structures

The predominant structures that arise from different optimization problems can significantly differ. More specifically, feed and cooling water flows can vary drastically among structures, which would make comparing structures based on GOR and SA alone, without considering variation in other operating costs, unjustified. Larger feed and cooling water flows increase operational costs through elevating both pretreatment costs and system pumping requirements. To minimize large discrepancies between structures and allow for more fair comparison, additional constraints are imposed.

The first constraint imposes that the recovery ratio (RR) in any structure is greater than or equal to 0.2, where the RR is defined as the fraction of the total feed to the system (less the cooling water) that is converted to distillate. Note that to attain minimum SA, optimization favors minimum RR, as allowed by the value of the GOR imposed. This is because a lower RR lowers the average salinity of the brine leaving each effect, thus reducing boiling point elevation (BPE) losses. Lower BPE losses in turn increase the prevalent temperature differential between the heating vapor and the brine being heated within each effect, thereby reducing area requirements. Low RR however detracts from distillate production capability of plants mainly by increasing feed sensible heating requirements, which alternatively could have been used to achieve further evaporation. Ultimately, for the lower GOR structures, the imposed inequality constraint is synonymous to setting the RR exactly to 0.2. For higher GOR structures, the constraint allows optimization to resort to higher RR values that allow for satisfaction of distillate requirements. Caution however must be taken when comparing structures of differing RRs, where additional merit must be given to those structures with higher RR, all things else equal.

The second constraint imposes that the maximum allowable cooling water to total distillate ratio (CW–TD ratio) is set to 4. From an exergy

**Table 2**
Properties of maximum GOR structures for the different vapor extraction locations.

| ES | $GOR_{max}$ | Ra | $P_{ev}$ | CR | $Tv_{12}$ | $T_{HS_1}$ | $T_{HS_1}-Tv_{12}$ | RR |
|---|---|---|---|---|---|---|---|---|
| 4 | 15.4 | 0.93 | 15.2 | 1.81 | 29.2 | 67.1 | 37.9 | 0.2 |
| 6 | 17.5 | 0.95 | 17.5 | 1.81 | 28.8 | 70.4 | 41.6 | 0.2 |
| 9 | **21.5** | 0.86 | 9.1 | 1.81 | 28.1 | 56.3 | 28.2 | 0.2 |
| 12 | 16 | 1.42 | 5.4 | 2.9 | 34.2 | 55.3 | 21.1 | 0.25 |

Maximum PR achievable.

accounting standpoint, allowing the brine blow-down to be outputted at a temperature very close to the seawater temperature is optimal. This arrangement however results in extremely large cooling water flow requirements. Generally availability of infinite cooling water can result in a simultaneous increase in distillate production (due to lower feed sensible heating requirements in last effect), and reduction in area requirements (larger possible average temperature difference between effects). Thus, restricting the amount of cooling water on a per unit of distillate production basis is a good mechanism to maintain a realistic operating plant. Although the CW–TD constraint is introduced as an inequality constraint, it is generally always satisfied with equality by the optimizer.

The methodology presented allows the introduction of additional constraints, such as for instance, imposing a minimal temperature for an effect.

## 5. Results and discussion

### 5.1. Intermediate vapor extraction increases maximum possible GOR

For a fixed flow rate of motive steam at a predesignated pressure, results confirm that intermediate vapor extraction increases the maximum distillation production. Among the 4 extraction options allowed in this study, Table 2 indicates that the maximum GOR is attained by the configuration with ES = 9 which is capable of 35% more distillate production compared to the maximum achievable amount by the conventional MED–TVC. The next best alternative is the structure with ES = 6, which itself is capable of achieving 10% additional distillate production. It is interesting to note that the optimal ES = 4 structure is unable to match the distillate production capacity of the conventional MED–TVC, for reasons to be discussed later in the section. From an implementation standpoint, structures represented by maximum distillate production must be avoided as they require near infinite areas. It is still instructive however to use highlight prevalent features of these structures that enhance their distillate production capability.

To lay the foundation for the subsequent analysis, it is important to realize that integration with thermal vapor compression in the traditional MED–TVC increases GOR compared to the conventional MED precisely because it enables the reuse of the vapor produced in the last effect as heating steam to all the effects that precede it. It does so by first increasing the amount of heating steam available to the 1st effect. This increases vapor production in the 1st effect which in turn increases vapor production in the 2nd effect. This trend continues up until the last effect. For increased distillate production goals, this is a much preferred scheme compared to the scheme common to the stand-alone MED, whereby most of the latent heat of the last effect vapor is transferred to cooling water that is eventually returned to the sea.

For a fixed supply of motive steam, it is intuitive that the entrainment of the largest amount vapor (i.e., low Ra) is desirable. Within steam ejectors, there is a prevalent trade-off between the amount of the low-pressure vapor that can be compressed, and the CR that results. Precisely, increasing amount of vapor entrained, decreases the CR. This analysis leads us to conclude that for the maximum GOR, the optimal structure should have the lowest allowable pressure ratio as allowed by the ejector. The previously discussed lower bound on the CR is 1.81.

The downfall of the conventional MED–TVC is that it extracts vapor at the lowest system pressure corresponding to the pressure existing in the last effect. Assuming that the last effect operates at a temperature slightly larger than the seawater temperature, a CR of 1.81 would result in a heating steam temperature that is not sufficiently elevated to drive a 12 effect MED. As an illustrative example, if the vapor pressure in the last effect is 4 kPa (corresponding to 30 °C temperature within the last effect), a CR of 1.81 would result in a heating steam temperature of approximately 40 °C. Given that the average BPE losses alone within each effect are approximately 0.8 °C, the total temperature difference is insufficient to drive heat transfer within 12 effects.

The intermediate vapor extraction scheme tackles this problem. By entraining vapors at higher pressures, it is possible to entrain the maximum amount of vapor as allowed by ejector operation. Table 2 confirms that for ES = 4, 6 and 9, the limiting factor to how much vapor can be entrained is the steam ejector operation limits, while for the case of ES = 12 the limiting factor is ensuring the optimal structure whereby there is both a sufficient temperature difference for heat transfer within each effect, while satisfying imposed constraints on how much cooling water can be utilized.

Variation in the maximum GOR among the different extraction locations can be attributed to the number of stages the entrained vapor is reused in. For the ES = 9 structure, the entrained vapor once compressed is used to generate additional vapor in the 1st effect through to the 9th effect. For the ES = 4 structure, however, the entrained vapor is only reused in the 1st effect through to the 4th effect. This explains why the ES = 4 structure, though capable of entraining more vapor, is still not capable of producing as much distillate as the conventional MED–TVC. In this light, it is predicted that for similar entrainment ratios, a larger maximum GOR is possible for structures with the later extraction stage as is confirmed in Table 2.

**Table 3**
Comparison of minimum SA ($m^2$ s/kg) at different GOR for different ES.

| ES | GOR = 10 | 11 | 12 | 13 | 14 | 15 | 16 | 17 | 18 | 19 |
|---|---|---|---|---|---|---|---|---|---|---|
| 4 | **262** | **297** | **332** | 380 | 459 | 768 | – | – | – | – |
| 6 | 269 | 299 | 335 | **377** | 418 | 478 | 555 | 710 | – | – |
| 9 | 275 | 314 | 344 | 378 | **416** | **461** | **521** | **601** | **711** | **866** |
| 12 | 333 | 359 | 457 | 606 | 823 | 1217 | 3357 | – | – | – |

Maximum PR achievable.

**Table 4**
Properties of optimal structures for GOR = 15 for different vapor extraction locations.

| ES | Ra | CR | $T_{HS_1}$ | $T_{v_{ext}}$ | $T_{v_{12}}$ | $\frac{T_{b_1}-T_{b_{ES}}}{ES-1}$ | $\frac{T_{b_{ES}}-T_{b_N}}{N-ES}$ | $\frac{T_{b_1}-T_{b_N}}{N-1}$ | SA |
|---|---|---|---|---|---|---|---|---|---|
| 4 | 0.97 | 1.81 | 73.1 | 59.6 | 29.4 | 3.2 | 3.8 | 3.7 | 768 |
| 6 | 1.08 | 2.02 | 72.4 | 56.6 | 30.6 | 2.5 | 4.5 | 3.6 | 477 |
| 9 | 1.73 | 3.17 | 72.5 | 47.6 | 30.6 | 2.7 | 5.1 | 3.6 | 461 |
| 12 | 1.67 | 3.4 | 56.6 | 32.9 | 32.9 | 2.0 | N/A | 2.0 | 1217 |

**Table 5**
Optimal structures corresponding to different ES for GOR = 15.

| ES | Structure |
|---|---|
| 4 | MED–TVC + MED + MSF |
| 6 | MED–TVC + MED + MSF |
| 9 | MED–TVC + MSF |
| 12 | MED–TVC |

**Table 6**
Optimal structures corresponding to different ES for maximum GOR.

| ES | Structure |
|---|---|
| 4 | MED–TVC + MED + MSF |
| 6 | MED–TVC + MED + MSF |
| 9 | MED–TVC + MSF |
| 12 | MED–TVC |

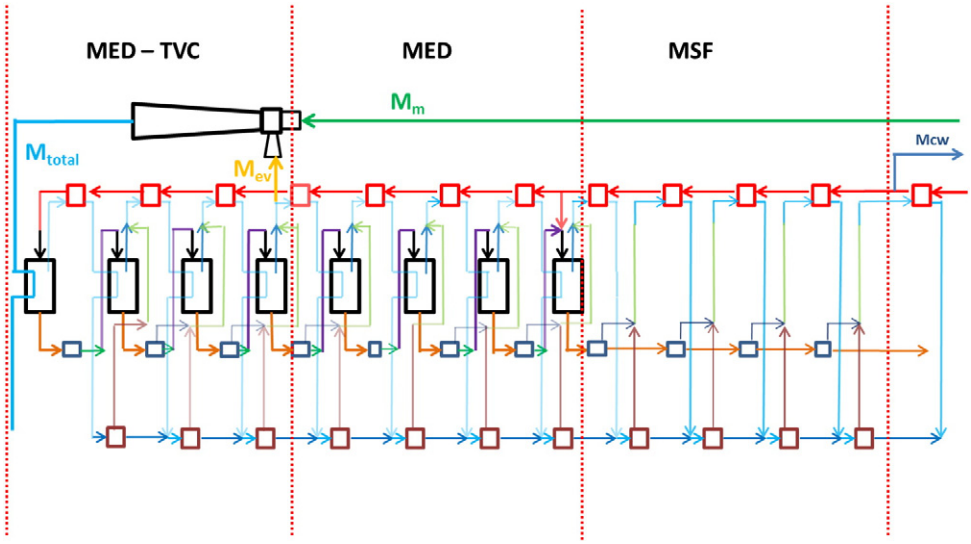


**Fig. 4.** Illustration of example of an MED–TVC + MED + MSF with vapor extraction at N = 4.

*5.2. Lower area requirements for structures with intermediate vapor compression*

The performed study confirms that the location from where the vapor is extracted for entrainment is an important consideration that not only affects the range of possible GOR, but also heavily influences the minimum SA requirements. Table 3 illustrates the results of the optimization of a 12 unit superstructure with vapor extractions from the 4th, 6th, 9th and 12th (last effect) respectively.

Further, the choice of the optimal location of vapor extraction is highly dependent on exact GOR requirements. It is observed that for lower range of GOR requirements ($10 \leq GOR \leq 12$), compression of a portion of vapor produced in the 4th unit is most favorable (ES = 4). For the higher range of GOR requirements ($13 \leq GOR \leq 16$), intermediate vapor extraction from later effects (ES = 9) is most advantageous. For all GOR requirements, the conventional MED–TVC (ES = 12) is undesirable; it requires 27 additional % SA requirements compared to ES = 4 for GOR = 10, double the SA requirements compared to ES = 9 for GOR = 14, and more than six times the SA requirements compared to ES = 9 for GOR = 16.

Using the case of GOR = 15, Table 4 highlights important parameters that can be compared to understand variation in the SA requirements between structures dependent on their extraction location. The parameter $\frac{T_{b_1}-T_{b_{ES}}}{ES-1}$ computes the average temperature difference in the effects that precede the compression, while $\frac{T_{b_{ES}}-T_{b_N}}{N-ES}$ computes the average available temperature difference in the possible effects/stages that follow vapor extraction. Finally, $\frac{T_{b_1}-T_{b_N}}{N-1}$ is used to compute the average temperature difference in the entire structure. Knowing available temperature differences is important since they heavily influence area requirements and help inform choice of hardware. For instance, MSF stages can approximately double distillate production with double the temperature difference. To a first order, however, MED effects do not benefit from additional temperature differences from a distillate production standpoint, though required heat transfer areas are reduced with larger temperature differences. The optimization formulation weighs all different choices to first ensure that distillate production requirements are met, and subsequently to ensure that it is done with the optimal component set that is least area intensive.

Intermediate vapor compression is found to reduce SA requirements for two main reasons. The first reason is that intermediate compression of vapor allows a larger fraction of the total heat transfer to occur in the initial effects (since more heating steam is available to the effects that precede extraction), which are characterized by the highest overall heat transfer coefficients. This is in contrast to the conventional MED–TVC where near equal amount of heat transfer occurs in all effects. The second reason is that intermediate compression enables larger ($T_{HS_1} - Tv_{12}$) factors as seen in Table 4, which allows a larger average temperature difference in the effects. This feature is

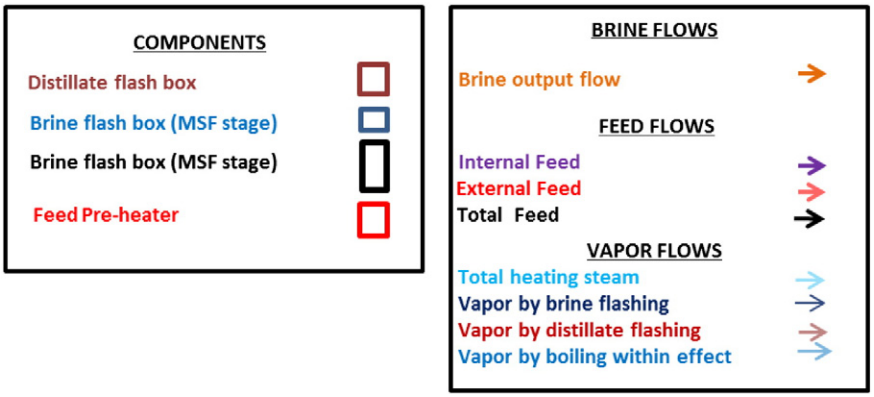


**Fig. 5.** Labeling of different flow streams.

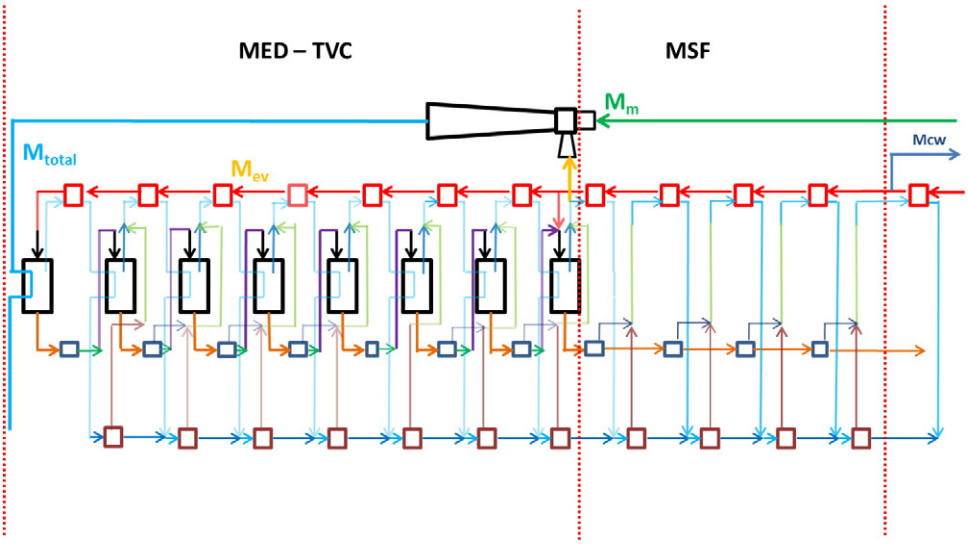


**Fig. 6.** Illustration of an example of an MED–TVC + MSF with vapor extraction at N = 8.

possible since the compression of higher pressure streams allows a higher heating steam temperature to the first effect. Moreover, low brine blow down temperatures can still be maintained, since the uncompressed vapor is still capable of driving a thermal desalination whereby the last effect can approach temperature of seawater, as allowed by cooling water requirements.

### 5.3. Optimal hybrid structures

The optimal hybrid structures take on varying forms depending on the location of vapor extraction as indicated in both Tables 5 and 6. To the authors' knowledge, none of these structures have been previously proposed in the literature. Schematics of the MED–TVC + MED + MSF and MED–TVC + MSF structures are presented in Figs. 4 and 6 respectively, while a clarification of the routing of the different flows within each of the structures as well as a justification of this naming is provided in Subsection 5.4. Simplified block-diagrams detailing the maximum GOR structures for ES = 6 and 9 can be found in Appendix A (Figs. 7 and 8).

### 5.4. Flowsheets of optimal hybrid structures

Within any superstructure unit, the input heating steam can be directed in three alternative feasible ways. The first choice involves sending all of the heating steam to the MED effect where it is responsible for vapor production. The second feasible option is to utilize the heating steam exclusively for feed pre-heating purposes. The final option is to allow a fraction of the heating steam to preheat the feed, while the other fraction is utilized to generate vapor in an MED effect.

The MED–TVC + MED + MSF structure, presented in Fig. 4, is such a structure which utilizes all the aforementioned options. In the effects that precede the extraction, a typical MED structure results. All the discharge steam exiting the steam ejector is directed towards vapor production in the 1st effect, while the intermediate generated vapors are split between feed pre-heating and vapor production. This part of the structure is referred to as the MED–TVC portion of the plant and includes both the steam ejector as well as all the effects leading up to and including the extraction stage. At the extraction stage, the generated vapor is split. The portion that is not entrained in the ejector serves as heating steam to a series of MED effects and their corresponding preheaters. This portion of the plant, made up of the unentrained vapor as well as the MED effects, is referred to as the MED portion of the plant. At a later stage, the structure transitions to yet another form, whereby all the generated vapor is dedicated solely for pre-heating purposes. This portion of the plant, which is devoid of any MED effects, produces vapor solely by brine and distillate flashing. As a result it is termed the MSF section of the plant. The integration of the three portions of the plant described is therefore termed the MED–TVC + MED + MSF structure. The MED–TVC + MSF structure, on the other hand, is represented in Fig. 6. The MED–TVC section portion of the plant is similar to that described earlier. At the extraction stage, however, all the unentrained vapor is directed completely towards preheating the feed. This represents the MSF section of the plant.

For both structures, the vapor produced in the last MSF stage is cooled in a down-condenser, whereby additional cooling water is inserted to remove any additional heat that cannot be carried away by the incoming feed. Moreover, for both structures, the routing of the feed is one such that all the incoming feed is inserted into one preheating line. Consequently, for the MED–TVC + MED + MSF structure, by the time the feed eventually enters into the MED–TVC section, it would already be significantly pre-heated by the vapor produced in both the MSF and MED sections that follow it. Similarly, the feed that enters the MED section is preheated in the MSF section. For the MED–TVC + MSF structure, the feed entering the MED–TVC section is preheated by the MSF structure. In both structures, the brine routing in the structures is such that the brine entering into the MSF stages is composed of brine streams exiting the earlier MED effects within the integrated structure.

### 5.5. Advantages of hybrid structures

Numerous benefits are associated with the hybridized schemes proposed. For instance, the feed pre-heating requirements in the MED–TVC section are greatly reduced owing to the fact that the feed enters the MED–TVC section at a temperature significantly elevated compared to the seawater temperature. This has the implication of increasing the vapor production in the initial MED effects, which translates into additional vapor production in the entire structure, thereby increasing GOR. Another notable advantage is that a significant reduction in the cooling water requirements is possible, resulting from the fact that only vapor produced by flashing in the last MSF section needs to be condensed, as compared to needing to condense the larger amount of vapor that would typically form in the more efficient boiling process which occurs with an MED effect. By setting a low temperature drop in the last

MSF stage of both plants, it is possible to greatly reduce the vapor flow that needs to be condensed. Given that the cooling water requirements in this study are fixed, this arrangement enables a lower increase in the temperature of the feed as it flows through the down condenser. This is desirable since it allows the last effects and stages to operate at lower temperature conditions, which both increases thermodynamic efficiency and reduces SA requirements in system by increasing the average temperature difference in the effects.

Additional advantages include an increased production of vapor by distillate flashing in both the MED and MSF sections, which is enabled by the large amount of distillate that is made available to the corresponding distillate flash boxes from the high distillate-producing MED–TVC section that precedes them. Finally, since the bulk of the total feed to the system is extracted to be fed to the MSF stages, the pumping requirements are expected to be significantly lower than what they alternatively would have been had all the feed been directed to the 1st effect; an arrangement where pressure losses would be large owing to the large amount of brine circulation required. This however, cannot be confirmed since pumping requirements are not directly computed in this work.

## 6. Conclusion

By optimizing a flexible superstructure allowing for multiple options for vapor extraction, several general conclusions stand out regarding the thermodynamic as well as economic advantages associated with intermediate vapor compression. From a thermodynamic standpoint, optimal structures with intermediate vapor compression were demonstrated to be capable of significantly larger GOR compared to an optimized conventional MED–TVC structure. From an economic standpoint, for a fixed GOR, optimal structures with intermediate vapor compression were shown to require lower SA requirements compared to the conventional MED–TVC structure. Another important finding is that there is no universally optimal location for vapor extraction. The optimal choice of extraction depends on the desired GOR and can only be attained through a full optimization as performed in this study.

More specifically, the global optimization enabled the identification of two novel structured configurations — the MED–TVC + MED + MSF and the MED–TVC + MSF. Both these structures are capable of satisfying large GOR demands, while simultaneously requiring low heat transfer areas and cooling water requirements.

*Nomenclature*

| *Variables* | Name of variable | Units |
|---|---|---|
| T | Temperature | K |
| P | Pressure | kPa |
| X | Salinity | g/kg |
| M | Heating steam to first effect | kg/s |
| HS | Heating steam to a superstructure unit | kg/s |
| CW | Cooling water | kg/s |
| *Subscript* | | |
| i | Component number | |
| ev | Entrained vapor | |
| s | Discharge vapor | |
| m | Motive steam | |
| ext | Extraction stage | |
| *Abbreviations* | | |
| FF | Forward feed | |
| PC | Parallel cross | |
| PF | Parallel feed | |
| TVC | Thermal vapor compression | |
| MSF | Multi-stage flash distillation | |
| MED | Multi-effect distillation | |
| *Parameters* | | |
| Ra | Entrainment ratio | Dimensionless |
| CR | Compression ratio | Dimensionless |
| ES | Extraction stage | |
| GOR | Gain output ratio | Dimensionless |
| RR | Recovery ratio | Dimensionless |
| SA | Specific heat transfer area requirements | $\frac{kgs}{m^2}$ |

## Acknowledgments

The authors would like to thank the King Fahd University of Petroleum and Minerals in Dhahran, Saudi Arabia, for funding this work through the Center for Clean Water and Clean Energy at MIT and KFUPM under project number R13-CW-10. We would like to also thank our colleagues at MIT and KFUPM for the useful discussions, in particular Gina M. Zak and Prof. John H. Lienhard V.

## Appendix A. Block diagrams for maximum GOR structures involving TVC

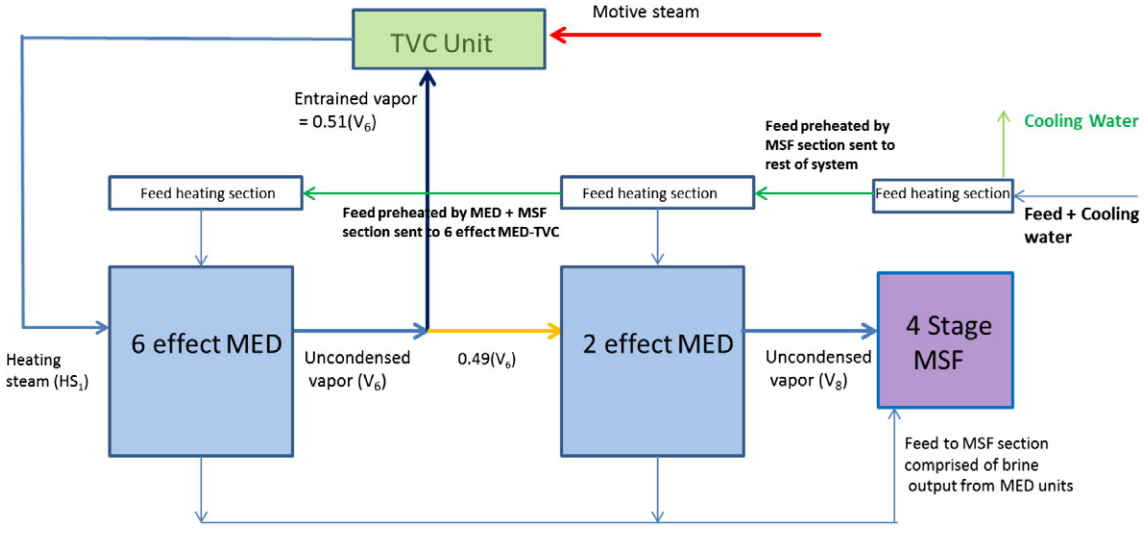


**Fig. 7.** Simplified block diagram to illustrate makeup of maximum GOR structure for ES = 6.

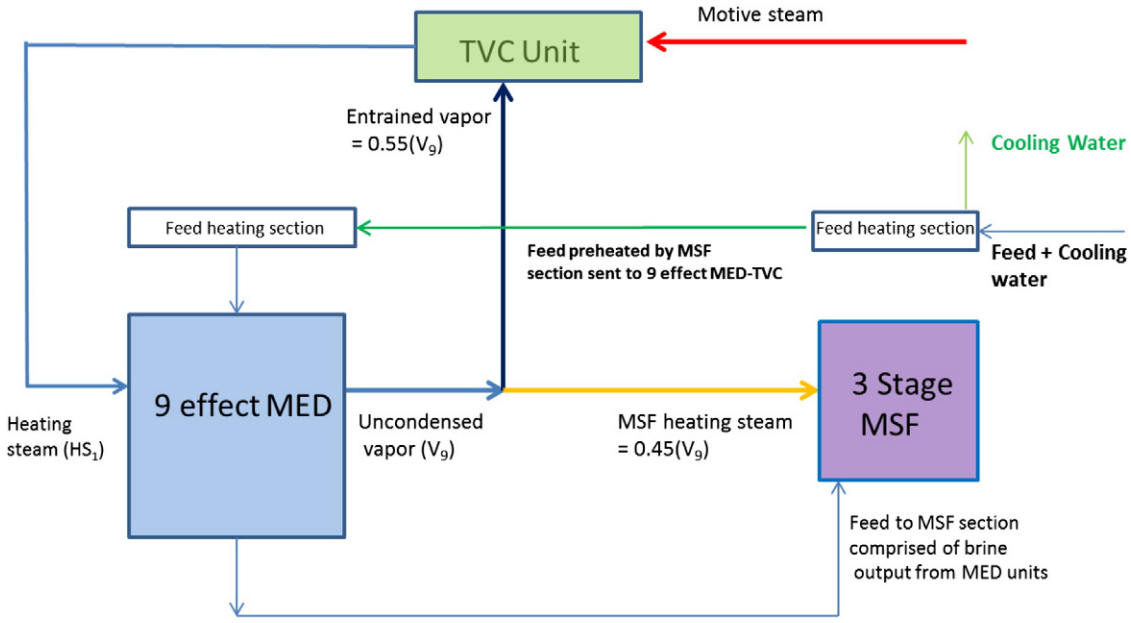


**Fig. 8.** Simplified block-diagram to illustrate makeup of maximum GOR structure for ES = 9.

## References


[1] N.M. Al-Najem, M.A. Darwish, F.A. Youssef, Thermo-vapor compression desalters: energy and availability — analysis of single and multi-effect systems, Desalination 110 (1997) 223–228.
[2] O.A. Hamed, A.M. Zamamiri, S. Aly, N. Lior, Thermal performance and exergy analysis of a thermal vapor compression desalination system, Energy Convers. Manag. 37 (1996) 379–387.
[3] A.O. Bin Amer, Development and optimization of ME-TVC desalination system, Desalination 249 (2009) 1315–1331.
[4] G.M. Zak, Thermal Desalination: Structural Optimization and Integration in Clean Power and Water, Master's thesis MIT, 2012.
[5] A. Al-Radif, Review of various combinations of a multiple effect desalination plant and a thermal vapour compression unit, Desalination 93 (1993) 119–125.
[6] S.E. Aly, Energy savings in distillation plants by using vapor thermo-compression, Desalination 49 (1984) 37–56 (S. E. Aly, Energy savings in distillation plants by using thermo-compression).
[7] T. Michels, Recent achievements of low temperature multiple effect desalination in the western areas of Abu Dhabi, Desalination 93 (1993) 111–118.
[8] M.A. Darwish, A. Alsairafi, Technical comparison between TVC/MEB and MSF, Desalination 170 (2004) 223–239.
[9] H. El-Dessouky, Modelling and simulation of the thermal vapour compression desalination process, Nucl. Desalin. Seawater (1997) 315–338.
[10] M. Shakouri, H. Ghadamian, R. Sheikholeslami, Optimal model for multi effect desalination system integrated with gas turbine, Desalination 260 (2010) 254–263.
[11] I.J. Esfahani, A. Ataei, V. Shetty, T. Oh, J.H. Park, C. Yoo, Modeling and genetic algorithm-based multi-objective optimization of the MED–TVC desalination system, Desalination 292 (2012) 87–104.
[12] F. Al-Juwayhel, H. El-Dessouky, H. Ettouney, Analysis of single-effect evaporator desalination systems combined with vapor compression heat pumps, Desalination 114 (1997) 253–275.
[13] D. Zhao, J. Xue, S. Li, H. Sun, Q. Zhang, Theoretical analyses of thermal and economical aspects of multi-effect distillation dealing with high-salinity wastewater, Desalination 273 (2011) 292–298.
[14] F. Mandani, H. El-Dessouky, H.M. Ettouney, Performance of parallel feed multiple effect evaporation system for seawater desalination, Appl. Therm. Eng. 20 (2000) 1679–1706.
[15] R.K. Kamali, A. Abbassi, S.A. Sadough, A simulation model and parametric study of MED–TVC process, Desalination 235 (2009) 340–351.
[16] F.N. Alasfour, M.A. Darwish, A.O. Bin Amer, Thermal analysis of ME-TVC + MEE desalination systems, Desalination 174 (2005) 39–61.
[17] M. Al-Salahi, H. Ettouney, Developments in thermal desalination processes: design, energy, and costing aspects, Desalination 214 (2007) 227–240.
[18] K.A. Ahmed, O.A. Hamed, An assessment of an ejectocompression desalination system, Desalination 96 (1994) 103–111.
[19] H. Sayyaadi, A. Saffari, A. Mahmoodian, Various approaches in optimization of multi effects distillation desalination systems using a hybrid meta-heuristic optimization tool, Desalination 254 (2010) 138–148.
[20] M.A. Sharaf, A.S. Nafey, L. Garcia-Rodrigues, Exergy and thermoeconomic analyses of a combined solar organic cycle with multi effect distillation (MED) desalination process, Desalination 272 (2011) 135–147.
[21] N. Lukic, A.P. Froba, L.L. Diezel, A. Leipertz, Economical aspects of the improvement of a mechanical vapor compression desalination plant by dropwise condensation, Desalination 264 (2010) 173–178.
[22] R.K. Kamali, A. Abbasi, S.A. Vanini, M.S. Avval, Thermodynamic design and parametric study of MED–TVC, Desalination 222 (2008) 596–604.
[23] H. Sayyaadi, A. Saffari, Thermoeconomic optimization of multi effect distillation desalination systems, Appl. Energy 87 (2010) 1122–1133.
[24] K. Ansari, H. Sayyaadi, H. Amidour, Thermoeconomic optimization of a hybrid pressurized water reactor (PWR) power plant coupled to a multi effect distillation system with thermo-vapor compressor (MED–TVC), Energy 35 (2010) 1981–1996.
[25] J. Ghelichzadeh, R. Derakhshan, A. Asadi, Application of alternative configuration of cogeneration plant in order to meet power and demand, Chem. Eng. Trans. 29 (2012) 775–780.
[26] R. Koukikamali, M. Senaei, M. Mehdizadeh, Process investigation of different locations of thermo-compressor suction in MED–TVC plants, Desalination 280 (2011) 134–138.
[27] H. El-Dessouky, H. Ettouney, L. Alatiqi, G. Al-Nuwaibat, Evaluation of steam jet ejectors, Chem. Eng. Process. 41 (2002) 551–561.
[28] N.H. Aly, A. Karameldin, M.M. Shamloul, Modelling and simulation of steam jet ejectors, Desalination 123 (1999) 1–8.
[29] R.K. McGovern, G.P. Narayan, J.H.V. Lienhard, Analysis of reversible ejectors and definition of an ejector efficiency, Int. J. Therm. Sci. 54 (2012) 153–166.
[30] A. Arbel, A. Shklyar, D. Hershgal, M. Barak, M. Sokolov, Ejector irreversibility characteristics, J. Fluids Eng. 125 (2003) 121–129.
[31] H.T. El-Dessouky, H.M. Ettouney, F. Al-Juwayhel, Multiple effect evaporation — vapour compression desalination processes, Chem. Eng. Res. Des. 78 (2000) 662–676.
[32] B.R. Power, Steam Jet Ejectors for Process Industries, 1, McGraw-Hill, 1994, pp. 1–494.
[33] N.V. Sahinidis, BARON: a general purpose global optimization software package, J. Glob. Optim. 8 (2) (1996) 201–205.
[34] M. Tawarmalani, N.V. Sahinidis, A polyhedral branch-and-cut approach to global optimization, Math. Program. 103 (2005) 225–249.
[35] N.V. Sahinidis, BARON: A general purpose global optimization software package, Journal of Global Optimization 8 (2) (1996) 201–205.
[36] M. Tawarmalani, N.V. Sahinidis, A polyhedral branch-and-cut approach to global optimization, Mathematical Programming 103 (2005) 225–249.